NREL
NATIONAL RENEWABLE ENERGY LABORATORY

Creep in Photovoltaic Modules: Examining the Stability of Polymeric Materials and Components

David C. Miller, Michael D. Kempe,
Stephen H. Glick, and Sarah R. Kurtz

Presented at the 35th IEEE Photovoltaic Specialists Conference (PVSC '10)
Honolulu, Hawaii
June 20-25, 2010

Conference Paper
NREL/CP-5200-47718
February 2011

Contract No. DE-AC36-08GO28308

NOTICE

Available electronically at http://www.osti.gov/bridge

Available for a processing fee to U.S. Department of Energy
and its contractors, in paper, from:

U.S. Department of Energy
Office of Scientific and Technical Information

P.O. Box 62
Oak Ridge, TN 37831-0062
phone: 865.576.8401
fax: 865.576.5728
email: mailto:reports@adonis.osti.gov

Available for sale to the public, in paper, from:

U.S. Department of Commerce
National Technical Information Service
5285 Port Royal Road
Springfield, VA 22161
phone: 800.553.6847
fax: 703.605.6900
email: orders@ntis.fedworld.gov
online ordering: http://www.ntis.gov/help/ordermethods.aspx

Cover Photos: (left to right) PIX 16416, PIX 17423, PIX 16560, PIX 17613, PIX 17436, PIX 17721

Printed on paper containing at least 50% wastepaper, including 10% post consumer waste.

CREEP IN PHOTOVOLTAIC MODULES: EXAMINING THE STABILITY OF POLYMERIC MATERIALS AND COMPONENTS

David C. Miller, Michael D. Kempe, Stephen. H. Glick, and Sarah R. Kurtz
National Renewable Energy Laboratory (NREL), 1617 Cole Boulevard, Golden, CO, USA 80401

ABSTRACT

Interest in renewable energy has motivated the implementation of new polymeric materials in photovoltaic modules. Some of these are non-cross-linked thermoplastics, in which there is a potential for new behaviors to occur, including phase transformation and visco-elastic flow. Differential scanning calorimetry and rheometry data were obtained and then combined with existing site-specific time-temperature information in a theoretical analysis to estimate the displacement expected to occur during module service life. The analysis identified that, depending on the installation location, module configuration and/or mounting configuration, some of the thermoplastics are expected to undergo unacceptable physical displacement. While the examples here focus on encapsulation materials, the concerns apply equally to the frame, junction-box, and mounting-adhesive technologies.

INTRODUCTION

Recent interest in renewable energy has motivated the implementation of new materials and components in photovoltaic (PV) modules. Ethylene-co-vinyl acetate (EVA) has historically been used to encapsulate the PV cell, whereas Poly(ethylene-co-methacrylic acid metal salt) (ionomer), Polyvinyl butyral (PVB), thermoplastic urethane (TPU), Poly-α-olefin (PO), and Poly(dimethylsiloxane) (PDMS) have been proposed for the same application. EVA, PO, and PDMS are thermosets (characterized by cross-linked networks). Ionomer, PVB, and TPU are thermoplastics (increasingly susceptible to visco-elastic flow as the temperature is increased above their glass- and melt-transition temperatures). Some other formulations of polyolefin, not examined in the study here, are thermoplastics. Regarding the non-traditional materials, PVB is commonly utilized in "impact-resistant" glass, ionomer has a low moisture diffusivity (possibly preventing corrosion), the low phase-transition temperatures for PO may favor it in a cold application site, and PDMS is both an exceptional optical transmitter and weather-resistant.

The melting temperature, T_m, glass-transition temperature, $T_g=T_\alpha$, at the α-relaxation, and β-relaxation temperature, T_β, are indicated in Figure 1. Also in the figure (note logarithmic scale), the viscosity, η, of a thermoplastic material may vary differently with temperature (slope m, where $m_1<m_2<m_3<m_4$) and exhibit discontinuity at phase transition events (ΔT^{-1}, $\Delta\eta$). In Figure 1, (m_1 and m_2), m_3, and m_4 correspond to the rubbery, glassy, and melt regimes, respectively. The magnitude and profile of such discontinuities depend upon the material. In particular, a "Williams-Landel-Ferry" (WLF) profile often exists for $T_g<T<T_g+100°C$ [1]. The magnitude of $\Delta\eta$ in such cases may be significant (see Figure 5 below), owing to the non-Arrhenius temperature dependence.

Polymeric materials are utilized in PV modules as encapsulation at the cell, as edge-seals (at the periphery), frames (at the periphery), junction-boxes, and structural sealants (mounting adhesives on the backside). Creep or loss of material at these locations may cause: motion/fracture of the internal active components, reduced electrical insulation/isolation, delamination at interfaces, increased moisture permeation (possibly rendering corrosion), loss of structural integrity, loss of connectivity (open circuits), exposed wires, compromised electronic grounding, electrical arcing, or falling components. These present serious risks to module performance, to operation, to the installation site (*e.g.,* fire), and/or to personnel. Secondary concerns include mechanical interaction between fallen/displaced modules (or components) and the installation site.

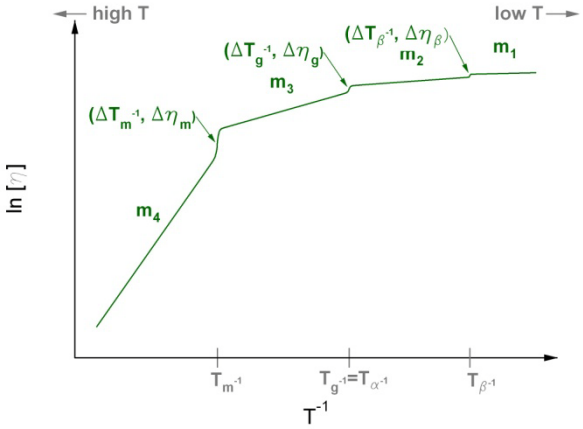

Figure 1 Schematic representing the variation in the rate of flow (viscosity, η) for a thermoplastic material as temperature is increased.

To explore these possible risks, phase transformation and creep were examined in the context of the flat-panel PV application for recently proposed polymeric materials. The goal of this study is to aid the PV industry in predicting creep-facilitated failure. The expected displacement related to encapsulation materials is used here as an example that may be applied more broadly, when selecting between polymeric materials or module designs. The work here is also intended to benefit module manufacturers and material vendors by providing the basis for a safety/qualification test that may be used for flat-panel PV modules.

THE APPLICATION ENVIRONMENT

To determine if a material is likely to creep, the expected service temperature conditions must be understood. In ref. [2], six different combinations of mounting- (roof and rack) and packaging-schemes (including glass/glass and glass/backsheet, represented using empirical models) were examined at multiple locations. The module temperature was estimated using the typical meteorological year (TMY3) data [3]. The results are shown in Figure 2 for roof-mounted modules, including the world's hottest cities (represented by Riyadh), another desert location (Phoenix), and a tropical (humid) location close to an ocean (Miami). The figure also indicates the maximum temperature, T_{max}, predicted for the sites during a typical year, listed in Table 1.

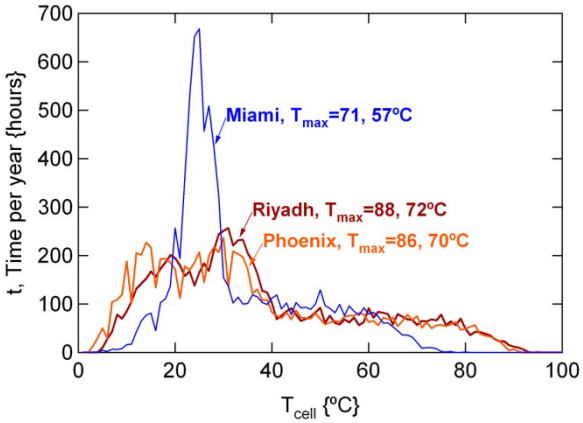

Figure 2 Time-temperature histograms (from [2], with 1ºC binning) of the cell in roof-mounted modules. T_{max} values are for roof and rack mounts, respectively.

Table 1 provides estimates of the maximum temperatures expected for modules at representative installation sites (ranked from hottest to coldest). In the table, the module construction is glass/glass for close-roof or open-rack mounting conditions, respectively. In close-roof mounting, a small air gap exists between the module and roof, with no insulation on the backside of the module. Close-roof mounting is 15±2°C (average ± 1 standard deviation) warmer than open-rack. The temperature estimates were obtained from analysis using the method described in ref. [2] for representative meteorological data (the "almanac" value for the maximum ambient temperature, T_{max}, during the hottest month) [4] and specific TMY3 (hourly averaged) data (*i.e.,* the maximum coincident irradiance and average wind-speed for the same hottest month). Irradiance values indicative of cloud brightening were excluded in the analysis.

It is also instructive to examine the maximum temperature for atypical (record hot) conditions. Table 2 predicts the maximum steady-state-equilibrated temperature for modules exposed to the record ambient conditions. To clarify, the record ambient temperature is used in Table 2, in conjunction with the maximum coincident irradiance (also used in Table 1) and assumed wind-speed of 0 m/s. Comparing Table 1 and Table 2, the record ambient T_{max}, [4] experienced over 20 or 30 years (the module service life) is 8±3°C warmer than the T_{max} observed in an average year. For the King models [2],[5], this results in a corresponding 10-20°C increase above the module-temperatures values in Table 1. The T_{max} of 85 or 90 °C is utilized in the present module qualification tests, *i.e.,* UL 1703, IEC 61215, and IEC 61646. The values in Table 2 are predicted (but not verified), whereas the values in Table 1 are expected to be experienced within PV modules during the typical year. Table 1 and Table 2 may eventually be compared to an on-going empirical study [6], utilizing a similar model (with different coefficients). Separately, the cell operating temperature in the table is known to be less than the temperature of the protection diodes during a reverse-current condition, occurring when the module is partially shaded. In that condition, the localized maximum temperature may exceed 140°C [7].

Table 1 Maximum operating cell temperature, predicted for a glass/glass module in two mounting configurations during a typical year [4] at each location.

LOCATION	T_{max}, ROOF {°C}	T_{max}, RACK {°C}	$T_{max, typical}$, AMBIENT {°C}
Death Valley, CA	97	80	47
Riyadh	88	72	44
Phoenix, AZ	86	70	42
Yuma, AZ	82	68	42
New Delhi	81	66	38
Seville	81	64	35
Kuwait City	81	67	44
Daytona, FL	74	59	33
Denver, CO	73	58	31
Miami, FL	71	57	32
Bangkok	71	58	35
New York, NY	68	54	29
Munich	59	46	22
Fairbanks, AK	53	42	23

Table 2 Maximum operating cell temperature, predicted for a glass/glass module using the maximum ambient temperature on record for each location.

LOCATION	T_{max}, ROOF {°C}	T_{max}, RACK {°C}	$T_{max, record}$, AMBIENT {°C}
Death Valley, CA	108	90	57
Riyadh	103	84	48
Phoenix, AZ	103	85	50
Yuma, AZ	100	83	51
New Delhi	97	79	45
Seville	97	79	45
Kuwait City	99	83	51
Daytona, FL	90	73	39
Denver, CO	89	72	40
Miami, FL	86	70	37
Bangkok	85	69	38
New York, NY	89	73	41
Munich	79	64	36
Fairbanks, AK	70	59	36

To compare the expected application environment to material behavior, the phase-transition temperatures, including the freezing temperature, T_f, for the encapsulation materials studied here are summarized in Table 3. The data were obtained for multiple PV-specific encapsulation formulations (where the number of formulations is indicated in parentheses in the table) using differential scanning calorimetry (DSC, Q1000, TA Instruments, Inc). The 2-Hz data were taken from the second of two consecutive cycles (from $-60 \le T \le 155$°C) at the rate of 10ºC/min in an N_2 environment. The average and standard deviation of the formulations considered is provided in Table 3. T_g was then also measured using dynamic mechanical analysis (DMA, Ares LS rheometer, TA Instruments, Inc.), indicated in parentheses. While T_g, T_m, or T_f may vary up to tens of degrees depending on the formulation, test rate, and/or measurement technique, the values in the table are considered representative. In hot locations such as those shown in Figure 2, all of these materials may experience temperatures above T_g; many exist above T_m. In Figure 1, significant flow may occur in either the glassy or melt regimes, m_3 or m_4. Therefore, Table 3 confirms that potentially adverse phase transitions may occur for the recently proposed materials, within the range of service temperatures encountered by PV modules, Figure 2, Table 1, and Table 2.

Table 3 Phase-transition temperatures, measured for encapsulation materials using DSC and DMA. DMA (torsional geometry at 15.9 Hz) results for T_g are indicated in parentheses.

MATERIAL (# OF FORMULATIONS)	T_g {°C}	T_f {°C}	T_m {°C}
IONOMER (2)	44±17 (69)	65±19	90±5
PVB (2)	19±5 (35)	N/A	N/A
TPU (3)	-11±32 (21)	N/A	N/A
EVA (2)	-34±0 (-16)	36±0	58±1
PO (1)	-57 (-35)	41	60
PDMS (4)	<-100	-72±7	-46±1

VISCOUS FLOW IN CONTEMPORARY MATERIALS

The non-cross-linked thermoplastics having the lowest phase-transition temperatures were measured in steady-state shear mode to determine their viscosity. For the measurements, the Ares LS instrument was equipped with a 25-mm diameter cone (cone angle of 0.0989 rad and 50.8 μm gap between the tip and 25-mm diameter plate). This method was used to produce viscosity vs. strain rate profiles at constant temperatures, shown in Figure 3 for an ionomer from 75-175°C. The measurements were first obtained for the applied shear of 100 and 1,000 Pa (averaged over the last 5 of 10 minutes) and then at the strain rates typically automated by the instrument (averaged for the last 1 of 3.5 minutes). An irregular profile was obtained at 75°C, suggesting the viscosity of the material exceeds the measurement capability at that temperature. Separately, a unique (parabolic) profile was repeatedly obtained at 175°C, suggesting the material was affected during the measurement performed at that temperature. For example, temperature induced cross-linking (or alternately, material degradation) could cause η to vary. Of the other profiles, data approaching $\gamma > 10^1$ s^{-1} identifies the rapid response, *e.g.,* approaching an impact event. In contrast, the data for $\gamma < 10^{-3}$ s^{-1} approaches the zero shear viscosity, which would be obtained for flow over prolonged time periods.

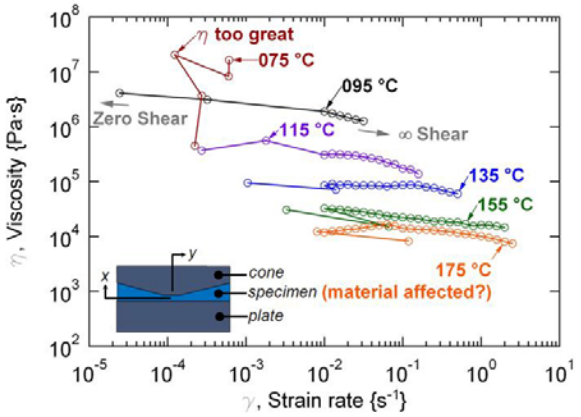

Figure 3 Viscosity, measured for an ionomer using DMA (cone/plate). The data at the 75 and 175 °C (found to be invalid) is included.

In Figure 3, measurements were made at an applied shear of 100 Pa, often approaching the zero shear viscosity. Those results are shown in Figure 4 for the non-cross-linked materials, where a least-squares fit is applied to the uniform data regions. Within each phase regime, the thermoplastics demonstrate Arrhenius-type profiles. Uncured EVA, which may occur as the result of expired curing agent or improper lamination, is expected to experience a far greater flow than the other materials in Figure 4 (note logarithmic scale). In the figure, ionomer, PVB, and TPU share similar viscosities. For these, the creep displacement will depend on the particular time-temperature history. For these materials, if a different material formulation were used, significantly different results could be obtained. The viscosity of cured EVA, PO, and PDMS is not indicated in Figure 4. These materials are cross-linked and therefore expected to yield, tear, or delaminate when loaded beyond a critical applied shear stress.

The data in Figure 4 are further summarized in Table 4, where the activation energy, E_a, is calculated from the linear fits. For comparison, the viscosity is tabulated in Table 4 at 100°C, a temperature that may be experienced by PV modules during record ambient temperatures, Table 2. The E_a values in Table 4, are consistent with the range $0.7 < E_a < 1.9$ eV, estimated from ref. [8] for the T_g of linear polymers for $-50 < T < 100$°C (*i.e.*, the temperature range likely to be present in the PV application). The E_a for uncured EVA, however, is notable greater.

While the data in Table 4 does not represent a comprehensive examination of each material type, it does allow for some comparisons. Foremost, until it began to cross-link during testing, uncured EVA proved to be the least viscous of the materials examined. This condition is largely theoretical, however, as EVA would be expected to cross-link while deployed at the application site (provided

the formulation has not expired). Alternately, because it is the least thermally activated (lowest E_a), the ionomer is the most difficult material to accelerate with temperature.

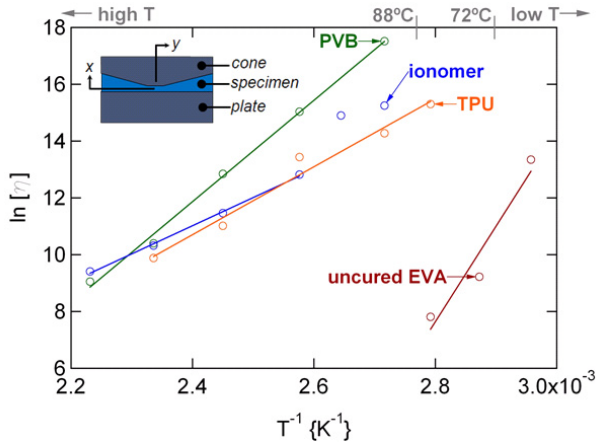

Figure 4 Viscosity, measured for encapsulation materials using DMA (cone/plate) as a function of temperature. The T_{max} for roof (88°C) and rack (72°C)-mounted modules in Riyadh, Table 1, is indicated.

Table 4 Analysis of E_a, from Figure 4. For the purpose of comparison, the viscosity (ln [η]) is estimated at 100°C.

MATERIAL	E_a, ACTIVATION ENERGY {eV}	ln [η], (@ 100°C)
IONOMER	0.9	13.8
TPU	1.0	14.0
PVB	1.5	16.9
EVA (UNCURED)	2.9	3.6

The linear fits in Figure 4 imply an Arrhenius-type relation between η and T. Such an assumption is valid as long as the material may be affected (equilibrated to temperature) homogeneously and a single mechanism dominates material behavior. Caution must be taken when such fits are extended beyond the range of their original characterization, as material degradation or phase transformation would render extrapolation invalid [9].

The Ares LS rheometer, and its chiller (Polycold, Helix Technology Corp.), were also utilized (from -60≤*T*≤135°C) with solid specimens of a rectangular geometry, as shown in Figure 5. For nominally 12.5 x 30.5 x 0.5-mm (width x length x thickness) specimens, data was obtained while heating from -60 to 135°C in a 1°C increment; a 1% oscillatory strain was applied along with a 20-g tensile load. DMA allows direct characterization of the mechanical response at lower temperatures. In the case of cross-linked materials (including cured EVA, PO, and PDMS), data may be obtained including the glassy, rubbery, and melt regimes. T_g and T_m, obtained using DSC for the same formulation, are indicated in Figure 5. T_g is determined to be -28, -16, and -33.6°C for DMA (@15.9 mHz), DMA (@15.9 Hz), and DSC (Table 3), respectively. The different values are a consequence of the different characterization methods and test rates utilized. DMA is fundamentally a mechanical test (arguably more similar to the PV application than DSC). In comparison, reported response times in modules include: resonant frequencies (1st and 2nd mode) on the order of 10-70 Hz [10] for wind load, time constants (1/τ for 1st order) on the order of 1-2·10^{-3} Hz [11],[12] for thermal transition (*e.g.*, thermal misfit occurring between the shaded and unshaded conditions), and time constants ($\tau_{0.5}$ for 1st order) on the order of 1·10^{-5} -1·10^{-8} Hz [13] for moisture ingress (*e.g.*, hydro-expansion occurring between dry and wet conditions). The results in Figure 5 therefore represent a thermal transient or externally applied load, respectively.

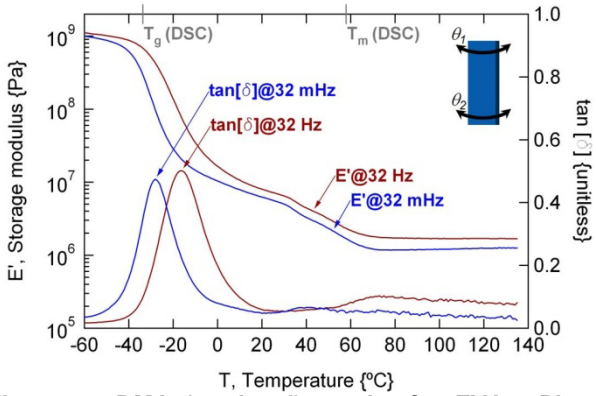

Figure 5 DMA (torsional) results for EVA. Phase transition temperatures (obtained using DSC, Table 3) are indicated at the top for comparison.

The shape of the profiles in Figure 5 may be compared to Figure 1. Despite the different parameters plotted in Figure 5, linear *E*' regions are evident for 30-60 and 70-135°C. The melt transition, occurring at their intersection, is therefore relatively discrete. In contrast, the glass transition is not only more distinct in magnitude (Δ*E*'), but occurs over a noticeable temperature range, *i.e.*, -50 to 30°C. The glass transition in Figure 5 therefore emphasizes the importance of phase transition, which in addition to creep may prove problematic for some thermoplastic polymeric materials. Note that the data in Figure 4, which utilizes a cone/plate test geometry, could be supplemented by that obtained using rectangular specimens (Figure 5) using the Cox-Mertz rules [14]. The extension of the viscosity profile to lower temperatures, however, was not explored in the work here.

ESTIMATING CREEP FROM MEASURED VISCOSITY

The creep expected during the service life of a PV module may be estimated from the measured viscosity. Using the front glass & encapsulation as an example, the key parameters related to creep are shown in Figure 6 for a glass/glass module package. In Figure 6 (a), the front glass is free to move relative to the back glass, whereas in Figure 6 (b) the glass at the front and back are constrained relative to each other. Key parameters in the figure, here for system international (SI) units, include: the displacement direction, *y* {m}, the external force, *F* {N}, the length of the area profile, *l* {m}, the width, *w* {m}, the tilt angle, θ {degrees}, the thickness, *h* {m}, material density, ρ {kg·m^{-3}}, gravitational acceleration, *g*=9.81 m·s^{-2}, the orthogonal direction, *x* {m}, the time, *t* {s}, and the

viscosity, η {Pa·s}. Subscripts *–g*, *-p* refer to the glass, and polymer, respectively. The example shown in Figure 6 for front glass & encapsulation could just as easily be applied to the situation of j-box & adhesive or module & adhesive.

Creep may be analyzed using Equation 1 and Equation 2 [15], which apply to the same configurations shown in Figure 6 (a) and (b), respectively. The same nomenclature is used for the figure and equations. The equations, which apply to Newtonian flow within a parallel plate configuration, are provided here to estimate displacement, ∂y {m}, as a function of time. More rigorous analysis accounting for the internal components (including cells, bus bars, and feed-throughs) using finite-element analysis for an Arrhenius or WLF (represented via Prony series) temperature dependence is not investigated here.

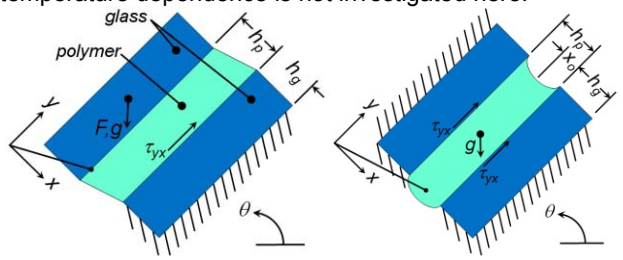

(a) (b)

Figure 6 Cross-sectional schematic, representing the geometry and factors involved in creep for the (a) fixed-free and (b) fixed-fixed boundary conditions.

$$\partial y = \frac{F \, l_g^{-1} \, w_g^{-1} \left(\sin\left[\theta\right]\right) + h_g \rho_g g \left(\sin\left[\theta\right]\right)}{\eta} \partial x \partial t \quad (1)$$

$$\partial y = \frac{\rho_p g \left(\sin\left[\theta\right]\right)}{2\eta} \left(x_o\right)^2 \partial t \quad (2)$$

Table 5 may be used with Equation 1 and Equation 2 to estimate creep, if the viscosity at a given temperature is known. The table provides order of magnitude values for "loads" (where $\tau_{yx}=F \cdot l^{-1} \cdot w^{-1}$), including: the self-weight of the polymeric encapsulation (at θ=45°), the weight of the front glass (at θ=45°), the pressure resulting from a person standing on a module (uniformly distributed across the front glass, at θ=45°), the weight of 5 meters of wire (10 or 12 AWG, which may exist between modules located at the same level), the weight of a small animal (which may rest upon a wire), and the self-weight of a module (uniformly distributed across the adhesive present, at θ=45°). The nomenclature for applicable systems includes: glass & encapsulant (*E*), polymeric frame (*F*), the junction-box (*J*), and the module & mounting adhesive (*M*). Regarding the values related to module size, they are estimated from the modules deployed at the National Renewable Energy Laboratory (NREL) Outdoor Test Facility. Table 5 (average±1 standard deviation) distinguishes between glass/backsheet (average $l^{-1} \cdot w^{-1}$=1.15±0.64 m^2) and glass/glass (average $l^{-1} \cdot w^{-1}$=0.91±0.44 m^2) package types, where 18 and 12 varieties were examined at NREL, respectively. Values related to personnel or animals represent unique events known to occur temporarily, but not necessarily during the hottest ambient conditions. The handling of a module by lifting at the wires (typically prohibited by the manufacturer, but sometimes realized temporarily during installation) is not considered in Table 5. The thermal stress associated with a hot-spot condition (not shown) is a temporary load condition. Based on the thermal misfit between the encapsulation and front glass, estimates of the τ present during reverse-current, range from kPa to MPa. Much of this stress, however, may be accommodated through strain-relief. In contrast, the self-weights of polymer, glass, wire, and modules represent loads present at all ambient conditions.

In Table 6, creep for the configurations shown in Figure 6, is analyzed (summed in 1°C increments) according to Equation 1 and Equation 2, respectively, using the measured viscosities from Figure 4, and time-temperature histories from the locations shown in Figure 2. The viscosity is assumed to be infinite below T_g (which would favor ∂y being underestimated). Likewise, for ionomer and uncured EVA, the viscosity is assumed to be infinite below T_m. While each configuration is assumed to be inclined at 45°, no external force is considered for either configuration. That is, τ_{yx} originates solely from the self-weight of the front glass in the case of Figure 6 (a), whereas τ_{yx} originates solely from the self-weight of the encapsulation for Figure 6 (b). Other key assumptions include: t_g=3.18 mm, ρ_g=2.52 g·cm^{-3}, ρ_p=0.95 g·cm^{-3}, and ∂x=2*x_o=1mm. (The original geometric mid-plane, x_o, occurs at the mid-thickness of the polymer).

Table 5 Representative (order of magnitude) load conditions that may be used to estimate creep in PV modules.

LOAD	SYSTEM	VALUE
encapsulation	E/F	τ=5 Pa
glass	E/F	τ=100 Pa
personnel (glass/backsheet)	E/F	τ=1000±600 Pa
personnel (glass/glass)	E/F	τ=1100±500 Pa
wire (5 m, 8-12 AWG)	J	*F*=5-20 N
animal (squirrel/raven)	J	*F*=5-15 N
module (glass/backsheet)	M	τ=900±100 Pa
module (glass/glass)	M	τ=2300±1100 Pa

The marked difference in ∂y for the thermoplastics in Table 6 despite their similar E_a values in Table 4 comes from their different phase-transition temperatures, Table 3. Further, Table 6 clearly shows that the fixed-free configuration, Figure 6 (a), is expected to demonstrate significant creep within 1 year, when close-roof mounted in Riyadh or Phoenix. Over the module service life of 30 years, the expected displacement for the thermoplastics (on the order of tens of millimeters) would be unacceptable. In practice, strain on the order of a millimeter could motivate the breaking of electrical interconnections, such as solder joints. A substantial reduction in ∂y is seen when the fixed-free configuration is rack-mounted, lowering the operating temperature. The significant improvement here might motivate distinction during module qualification, based on mounting configuration. The cooler temperatures associated with the

rack-mounted configuration, however, do not entirely alleviate concerns for PVB and TPU, where ∂y on the order of millimeters may occur during the service life. The same polymers, however, are expected to prove suitable in the fixed-fixed configuration, Figure 6 (b). This identifies the merit of module design (including components such as a frame or clips), which may enable the use of novel thermoplastic materials. The module design could, however, still prove problematic if the quality of manufacture became compromised. The low anticipated ∂y in Miami alternately suggests that the time-temperature history specific to each location (desert vs. non-desert) may prevent creep, possibly meriting a distinction between locations during module qualification. Uncured EVA, shown to be relatively non-viscous in Figure 4, would not be suitable in any circumstance. Cured EVA, PO, and PDMS are suitable in all applications – their cross-linked structure prohibits creep.

CONCLUSIONS

To better understand anticipated issues, phase transformation and creep were examined in the context of the flat-panel PV application for recently proposed polymeric materials. Module (cell) temperatures as hot as 85-100°C (exceeding that examined in the present qualification tests) were shown to be expected for glass/glass modules. Phase change, including glass- and melt-transitions, were therefore found to occur within the range of operating temperatures expected for PV modules. Using the site-specific time-temperature profile, the measured viscosity, and expected load conditions, the creep strain may be predicted using first principles-estimates. In the example here, creep in several thermoplastic encapsulation materials is expected to be problematic in glass/glass modules, when no frame or clips are used. The particular mounting configuration (roof or rack) and application site may also greatly affect (eliminate) creep. The methods here may be applied to polymers utilized in PV encapsulation, frame, junction-box, and mounting adhesive technologies. Based on the geometry and/or loads present, future study related to creep is recommended at the junction box and structural sealant (mounting adhesive).

ACKNOWLEDGEMENTS

This work was supported by the U.S. Department of Energy under Contract No. DE-AC36-08-GO28308 with the National Renewable Energy Laboratory.

REFERENCES

[1] P.R. Higgenbotham-Bertolucci, H. Gao, J.P. Harmon, "Creep and Stress Relaxation in Methacrylate Polymers: Two Mechanisms of Relaxation Behavior Across the Glass Transition Region", Polym. Eng. Sci., 41, 2001, 873-880.

[2] S. Kurtz, K. Whitfield, G. TamizhMani, M. Koehl, D. Miller, J. Joyce, J. Wohlgemuth, N. Bosco, M. Kempe, and T. Zgonena, "Evaluation of High-Temperature Exposure of Photovoltaic Modules", *in review*.

[3] http://rredc.nrel.gov/solar/old_data/nsrdb/1991-2005/tmy3/

[4] http://www.weatherbase.com/

[5] D.L. King, W.E. Boyson, and J.A. Kratochvil, "Photovoltaic Array Performance Model," Report No. SAND2004-3535, 2004.

[6] B.L. Shrestha, E.G. Palomino, and G. TamizhMani, "Temperature of Rooftop Photovoltaic Modules: Air Gap Effects", Proc. SPIE, 7412, 2009, 74120E.

[7] J.H. Wohlgemuth, D.W. Cunningham, A. Nguyen, G. Kelly, and D. Amin, "Failure Modes of Crystalline Si Modules", Proc. Photovoltaic Module Rel. Work., 2010.

[8] http://www.dowcorning.com/content/sitech/sitechms/

[9] P. Budrugeac, and E. Segal, "Some Problems Concerning the Compensation Effect in the Kinetics of the Thermal Degradation of Polymers", J. Thermal Anal., 39, 1993, 1199-1208.

[10] K.-A. Weiss, M. Assmus, S. Jack, and K. Koehl, "Measurement and Simulation of Dynamic Mechanical Loads on PV-Modules", Proc. SPIE, 7412, 2009, 741203.

[11] D.L. King, J.A. Kratochvil, and W.E. Boyson, "Temperature Coefficients for PV Modules and Arrays: Measurement Methods, Difficulties, and Results", Proc. IEEE PVSC, 1997, 1183-1186.

[12] D.C. Miller, N. Bosco, J.A. DelCueto, J.-W. Oh, and G. TamizhMani, *unpublished results*.

[13] M.D. Kempe, "Modeling Rates of Moisture Ingress into Photovoltaic Modules", Solar Energy Mats. Solar Cells, 90, 2006, 2720-2738.

[14] K.P. Menard, Dynamic Mechanical Analysis, CRC Press: Boca Raton, 1999.

[15] C.J. Geankoplis, Transport Processes and Separation Process Principles, Prentice-Hall: London, 2008.

Table 6 Physical displacement (creep) estimated for configurations shown in Figure 6, and measured viscosities from Figure 4. Comparison is made between 1 and 30 years (note different scale) for 3 representative locations.

	∂y, roof-mount, fixed-free, (Equation 1)			∂y, rack-mount, fixed-free (Equation 1)			∂y, roof-mount, fixed-fixed (Equation 2)		
	{mm/year}			{mm/year}			{μm/30 years}		
MATERIAL	Riyadh	Phoenix	Miami	Riyadh	Phoenix	Miami	Riyadh	Phoenix	Miami
PVB	0.7	0.6	0.1	0.1	0.1	0.0	0.3	0.3	0.0
IONOMER	10.3	6.4	0.0	0.0	0.0	0.0	4.6	2.8	0.0
TPU	31.3	27.6	6.5	7.9	6.7	2.1	13.9	12.3	2.9
EVA (UNCURED)	6.3E+04	4.3E+04	5.4E+02	7.4E+02	4.9E+02	7.6E-01	2.8E+04	1.9E+04	2.4E+02

REPORT DOCUMENTATION PAGE

Form Approved
OMB No. 0704-0188

PLEASE DO NOT RETURN YOUR FORM TO THE ABOVE ORGANIZATION.

1. REPORT DATE *(DD-MM-YYYY)*	2. REPORT TYPE	3. DATES COVERED *(From - To)*
February 2011	Conference Paper	

4. TITLE AND SUBTITLE
Creep in Photovoltaic Modules: Examining the Stability of Polymeric Materials and Components

5a. CONTRACT NUMBER
DE-AC36-08GO28308

5b. GRANT NUMBER

5c. PROGRAM ELEMENT NUMBER

6. AUTHOR(S)
D.C. Miller, M.D. Kempe, S.H. Glick, and S.R. Kurtz

5d. PROJECT NUMBER
NREL/CP-5200-47718

5e. TASK NUMBER
PVD9.1320

5f. WORK UNIT NUMBER

7. PERFORMING ORGANIZATION NAME(S) AND ADDRESS(ES)
National Renewable Energy Laboratory
1617 Cole Blvd.
Golden, CO 80401-3393

8. PERFORMING ORGANIZATION REPORT NUMBER
NREL/CP-5200-47718

9. SPONSORING/MONITORING AGENCY NAME(S) AND ADDRESS(ES)

10. SPONSOR/MONITOR'S ACRONYM(S)
NREL

11. SPONSORING/MONITORING AGENCY REPORT NUMBER

12. DISTRIBUTION AVAILABILITY STATEMENT
National Technical Information Service
U.S. Department of Commerce
5285 Port Royal Road
Springfield, VA 22161

13. SUPPLEMENTARY NOTES

14. ABSTRACT *(Maximum 200 Words)*
Interest in renewable energy has motivated the implementation of new polymeric materials in photovoltaic modules. Some of these are non-cross-linked thermoplastics, in which there is a potential for new behaviors to occur, including phase transformation and visco-elastic flow. Differential scanning calorimetry and rheometry data were obtained and then combined with existing site-specific time-temperature information in a theoretical analysis to estimate the displacement expected to occur during module service life. The analysis identified that, depending on the installation location, module configuration and/or mounting configuration, some of the thermoplastics are expected to undergo unacceptable physical displacement. While the examples here focus on encapsulation materials, the concerns apply equally to the frame, junction-box, and mounting-adhesive technologies.

15. SUBJECT TERMS
photovoltaic; PV

16. SECURITY CLASSIFICATION OF:			17. LIMITATION OF ABSTRACT	18. NUMBER OF PAGES	19a. NAME OF RESPONSIBLE PERSON
a. REPORT	b. ABSTRACT	c. THIS PAGE			19b. TELEPHONE NUMBER (*Include area code*)
Unclassified	Unclassified	Unclassified	UL		

Standard Form 298 (Rev. 8/98)
Prescribed by ANSI Std. Z39.18